

Arbitrarily high-order energy-preserving schemes for the Camassa-Holm equation

Chaolong Jiang¹, Yushun Wang², Yuezheng Gong^{3*}

¹ School of Statistics and Mathematics,

Yunnan University of Finance and Economics, Kunming 650221, P.R. China

² Jiangsu Provincial Key Laboratory for NSLSCS,

School of Mathematical Sciences, Nanjing Normal University,

Nanjing 210023, China

³ College of Science,

Nanjing University of Aeronautics and Astronautics, Nanjing 210016, P.R. China

Abstract

In this paper, we develop a novel class of arbitrarily high-order energy-preserving schemes for the Camassa-Holm equation. With the aid of the invariant energy quadratization approach, the Camassa-Holm equation is first reformulated into an equivalent system with a quadratic energy functional, which inherits a modified energy conservation law. The new system are then discretized by the standard Fourier pseudo-spectral method, which can exactly preserve the semi-discrete energy conservation law. Subsequently, the Runge-Kutta method and the Gauss collocation method are applied for the resulting semi-discrete system to arrive at some arbitrarily high-order fully discrete schemes. We prove that the schemes provided by the Runge-Kutta method with the certain condition and the Gauss collocation method can conserve the discrete energy conservation law. Numerical results are addressed to confirm accuracy and efficiency of the proposed schemes.

AMS subject classification: 65M12, 65M15, 65M70

Keywords: Invariant energy quadratization approach, Camassa-Holm equation, high-order energy-preserving scheme.

1 Introduction

In this paper, we consider the following Camassa-Holm (CH) equation [6, 7]

$$u_t - u_{xxt} + 3uu_x - 2u_xu_{xx} - uu_{xxx} = 0, \quad (x, t) \in \Omega \times (0, T], \quad (1.1)$$

with the periodic boundary condition

$$u(x + L, t) = u(x, t), \quad (x, t) \in \Omega \times [0, T],$$

and the initial condition

$$u(x, 0) = u_0(x), \quad x \in \Omega,$$

where $\Omega = [a, a + L]$ is a bounded domain. The CH equation arises as a model for the propagation of unidirectional shallow water waves, with $u(x, t)$ representing the height

*Correspondence author. Email: gongyuezheng@nuaa.edu.cn.

of the fluid free surface above a flat bottom. Under the periodic boundary condition, the CH equation possesses the following conserved quantities

$$\mathcal{M} = \int_{\Omega} u dx, \quad \mathcal{I} = \int_{\Omega} (u^2 + u_x^2) dx, \quad \mathcal{H} = -\frac{1}{2} \int_{\Omega} (u^3 + uu_x^2) dx, \quad (1.2)$$

where \mathcal{M} , \mathcal{I} and \mathcal{H} correspond to mass, momentum and Hamiltonian energy of the original problem, respectively.

There have been a large number of researches about the analysis and numerical solution of the CH equation in the literature. Constantin and Escher [14] showed that the solution of the CH equation could develop singularities at a finite time, even for smooth initial data value with compact support. Li and Olver [28] established the local well-posedness of the CH equation in the nonhomogeneous Sobolev space H^s with $s > 3/2$. Numerical strategies for solving the CH equation include finite difference methods [10, 23], pseudo-spectral methods [27, 24], local discontinuous Galerkin method [40], operator splitting methods [5, 16], multi-symplectic methods [12, 13, 44] and other effective methods (e.g., see Refs. [8, 17]). However, the mentioned methods cannot exactly preserve the energy of the original system.

It is well known that the energy conservation is an important property of Hamiltonian partial differential equations (PDEs). In Ref. [32], Matsuo et al. presented an energy-conserving Galerkin scheme for the CH equation. Gong and Wang constructed an energy-preserving wavelet collocation scheme for the CH equation [18]. Other energy-preserving schemes can be found in Refs. [15, 31]. However, the existing energy-preserving schemes have only second order in time, which can't provide satisfactory solutions in long time simulations with a given large time step. Therefore, one wants to obtain accurate solutions in the long-term computing, the time step has to be refined, which leads to expensive costs. To remove such obstacle, the most commonly used approach is to construct higher-order energy-preserving schemes, which make large marching steps practical while preserving the accuracy. To our best knowledge, there has been no reference considering a high-order energy-preserving scheme for the CH equation.

In [34], Quispel and McLaren derived third- and fourth-order average vector field (AVF) methods. Subsequently, Li, Wang and Qin [29] have extended the fourth-order AVF method to sixth order. At present, high-order AVF methods have been successfully applied to develop high-order energy-preserving schemes for Hamiltonian PDEs (e.g., see [4, 26]). For linear problems, the proposed high-order schemes are concise and a customized fast solver has been presented to solve the resulting discrete linear equations efficiently [26]. However, since high-order AVF methods require to calculate high-order derivatives of the vector field, the resulting schemes are tedious for nonlinear problems, such as the CH equation. Based on the method of discrete line integral, Brugnano et al. [3] proposed Hamiltonian Boundary Value Methods (HBVMs), which can be recast as a multistage Runge-Kutta (RK) method. HBVMs are of arbitrarily high order and can exactly preserve energy of polynomial Hamiltonian systems. For non-polynomial cases, a practical energy-preserving scheme is usually gained in the sense that the energy error remains bounded within machine precision, but one has to increase RK stages [2]. Recently, energy-preserving continuous stage RK (CSRK) methods have been attracting a lot of interest [21, 30, 33, 38]. This kind of methods can eliminate the limit of HBVMs to cover non-polynomial Hamiltonian systems. However, the implementation of the CSRK method requires the computation of integrals. If the appearing integrals are replaced by a fixed high-order quadrature, the resulting method is closely related to HBVMs [21]. In addition, the above mentioned high-order energy-preserving methods are only valid for Hamiltonian systems with constant skew-symmetric structural matrix.

For Hamiltonian systems with non-canonical structure matrix, these methods should be further discussed (e.g., see [1, 11, 39]).

In this paper, we present a novel strategy for efficiently developing arbitrarily high-order energy-preserving schemes for the CH equation. It is worth noting that the high-order numerical strategy can be generalized for general Hamiltonian system. We first utilize the invariant energy quadratization (IEQ) approach [20, 41, 42, 43] to transform the CH equation into an equivalent system, which possesses a quadratic energy functional and admits a modified energy conservation law. Then, the transformed system is discretized in space by the standard Fourier pseudo-spectral method. Subsequently, a class of arbitrarily high-order fully discrete schemes are derived by applying the RK method with some certain coefficient conditions and the Gauss collocation method in time, respectively. The newly proposed schemes have several desired advantages: (i) they are energy-preserving and can reach arbitrarily high-order; (ii) the required RK stages are optimal; (iii) they can eliminate the limit of HBVMs to cover non-polynomial cases; (iv) they can be directly applied for efficiently solving non-canonical Hamiltonian PDEs.

The rest of the paper is organized as follows. In Section 2, we present an equivalent reformulation of the CH equation based on the IEQ approach. In Section 3, a semi-discrete system with an energy conserving property is obtained by using the standard Fourier pseudo-spectral method for the spatial discretization. In Section 4, we apply high-order structure-preserving methods for the semi-discrete system to arrive at fully discrete schemes, which are shown to be energy-preserving as well. Several numerical experiments are presented in Section 5. We draw some conclusions in Section 6.

2 Model reformulation using the IEQ approach

In this section, we reformulate the CH equation into an equivalent form with a quadratic energy functional, which is called the IEQ reformulation. The IEQ reformulation for the CH equation provides an elegant platform for efficiently developing arbitrarily high-order energy-preserving schemes.

Firstly, Eq. (1.1) can be rewritten equivalently into the following Hamiltonian system

$$\frac{\partial u}{\partial t} = \mathcal{D} \frac{\delta \mathcal{H}}{\delta u}, \quad (2.1)$$

where $\mathcal{D} = (1 - \partial_{xx})^{-1} \partial_x$ is a skew-adjoint operator, \mathcal{H} is the Hamiltonian energy

$$\mathcal{H} = \int_{\Omega} H(u, u_x) dx, \quad H(u, u_x) = -\frac{1}{2}(u^3 + uu_x^2),$$

and $\frac{\delta \mathcal{H}}{\delta u}$ denotes the variational derivative of \mathcal{H} with respect to u

$$\frac{\delta \mathcal{H}}{\delta u} = \frac{\partial H}{\partial u} - \frac{\partial}{\partial x} \frac{\partial H}{\partial u_x} = -\frac{3}{2}u^2 - \frac{1}{2}u_x^2 + (uu_x)_x.$$

One intrinsic property of (2.1) is the energy conservation law

$$\frac{d}{dt} \mathcal{H} = \left(\frac{\delta \mathcal{H}}{\delta u}, \frac{\partial u}{\partial t} \right) = \left(\frac{\delta \mathcal{H}}{\delta u}, \mathcal{D} \frac{\delta \mathcal{H}}{\delta u} \right) = 0, \quad (2.2)$$

where (\cdot, \cdot) is the L^2 -inner product defined by $(f, g) = \int_{\Omega} fg dx$.

Next, we introduce the IEQ approach to reformulate the system (2.1). Let

$$q = g(u, u_x) = -\frac{1}{2}(u^2 + u_x^2),$$

then the Hamiltonian energy functional can be rewritten as

$$\mathcal{H} = \int_{\Omega} u q dx. \quad (2.3)$$

According to energy variational, the system (2.1) can be reformulated into the following equivalent form

$$\begin{cases} \partial_t u = \mathcal{D} \left(q + u \frac{\partial g}{\partial u} - \partial_x \left(u \frac{\partial g}{\partial u_x} \right) \right), \\ \partial_t q = \frac{\partial g}{\partial u} u_t + \frac{\partial g}{\partial u_x} \partial_x u_t, \end{cases} \quad (2.4)$$

with consistent initial conditions

$$u(x, 0) = u_0(x), \quad q(x, 0) = -\frac{1}{2}(u(x, 0)^2 + u_x(x, 0)^2),$$

where

$$\frac{\partial g}{\partial u} = -u, \quad \frac{\partial g}{\partial u_x} = -u_x.$$

Theorem 2.1. *The system (2.4) satisfies the following energy conservation law*

$$\frac{d}{dt} \mathcal{H} = 0, \quad \mathcal{H} = \int_{\Omega} u q dx.$$

Proof. By some calculations, we obtain from the system (2.4)

$$\begin{aligned} \frac{d}{dt} \mathcal{H} &= (u_t, q) + (u, q_t) \\ &= (u_t, q) + \left(u, \frac{\partial g}{\partial u} u_t + \frac{\partial g}{\partial u_x} \partial_x u_t \right) \\ &= (u_t, q) + \left(u \frac{\partial g}{\partial u}, u_t \right) - \left(\partial_x \left(u \frac{\partial g}{\partial u_x} \right), u_t \right) \\ &= \left(q + u \frac{\partial g}{\partial u} - \partial_x \left(u \frac{\partial g}{\partial u_x} \right), u_t \right) \\ &= \left(q + u \frac{\partial g}{\partial u} - \partial_x \left(u \frac{\partial g}{\partial u_x} \right), \mathcal{D} \left(q + u \frac{\partial g}{\partial u} - \partial_x \left(u \frac{\partial g}{\partial u_x} \right) \right) \right) \\ &= 0. \end{aligned}$$

This completes the proof. □

3 Structure-preserving spatial discretization

Many energy-preserving schemes have been designed and investigated for solving the CH equation in the literature, but little attention is paid to the energy-preserving properties brought by spatial discretization. In this section, the Fourier pseudo-spectral method is applied for the CH equation to derive a spatial semi-discrete scheme, which is shown to preserve the semi-discrete energy conservation law.

Let $\Omega_h = \{x_j | x_j = a + jh, 0 \leq j \leq N\}$ be a partition of $\Omega = [a, a + L]$ with mesh size $h = L/N$, where N is an even number. A discrete mesh function $U_j = U(x_j)$, $j \in \mathbb{Z}$ satisfies the periodic boundary condition if and only if

$$U_j = U_{j+N}. \quad (3.1)$$

Let $\mathbb{V}_h = \{\mathbf{U} | \mathbf{U} = (U_0, U_1, \dots, U_{N-1})^T\}$ be the space of mesh functions on Ω_h and satisfy the periodic boundary condition (3.1). We define the discrete inner product as follows

$$\langle \mathbf{U}, \mathbf{V} \rangle_h = h \sum_{j=0}^{N-1} U_j V_j, \quad \forall \mathbf{U}, \mathbf{V} \in \mathbb{V}_h.$$

The discrete L^∞ -norm of $\mathbf{U} \in \mathbb{V}_h$ is defined as

$$\|\mathbf{U}\|_{h,\infty} = \max_{0 \leq j \leq N-1} |U_j|.$$

In addition, we denote ‘ \cdot ’ as the componentwise product of vectors $\mathbf{U}, \mathbf{V} \in \mathbb{V}_h$, that is,

$$\mathbf{U} \cdot \mathbf{V} = (U_0 V_0, U_1 V_1, \dots, U_{N-1} V_{N-1})^T.$$

For brevity, we denote $\underbrace{\mathbf{U} \cdot \dots \cdot \mathbf{U}}_p$ as \mathbf{U}^p .

Let $S'_N = \text{span}\{g_j(x), 0 \leq j \leq N-1\}$ be the interpolation space, where $g_j(x)$ is trigonometric polynomials of degree $N/2$ given by

$$g_j(x) = \frac{1}{N} \sum_{l=-N/2}^{N/2} \frac{1}{a_l} e^{il\mu(x-x_j)},$$

with $a_l = \begin{cases} 1, & |l| < \frac{N}{2}, \\ 2, & |l| = \frac{N}{2}, \end{cases}$ and $\mu = \frac{2\pi}{L}$. We define the interpolation operator $I_N : C(\Omega) \rightarrow S'_N$ as follows [9]

$$I_N U(x) = \sum_{j=0}^{N-1} U_j g_j(x),$$

where $U_j = U(x_j)$. Taking the derivative with respect to x , and then evaluating the resulting expressions at the collocation point x_j , we have

$$\frac{\partial^s I_N U(x_j)}{\partial x^s} = \sum_{k=0}^{N-1} U_k \frac{d^s g_k(x_j)}{dx^s} = [\mathbf{D}_s \mathbf{U}]_j, \quad \mathbf{U} \in \mathbb{V}_h,$$

where $j = 0, \dots, N-1$ and \mathbf{D}_s is an $N \times N$ matrix with elements given by

$$(\mathbf{D}_s)_{j,k} = \frac{d^s g_k(x_j)}{dx^s}, \quad j, k = 0, 1, \dots, N-1.$$

Especially, for first and second derivatives, we have

$$\frac{\partial I_N U(x_j)}{\partial x} = [\mathbf{D}_1 \mathbf{U}]_j, \quad \frac{\partial^2 I_N U(x_j)}{\partial x^2} = [\mathbf{D}_2 \mathbf{U}]_j, \quad j = 0, 1, \dots, N-1,$$

where \mathbf{D}_1 is a real skew-symmetric matrix, and \mathbf{D}_2 is a real symmetric matrix. We note that [35]

$$\mathbf{D}_1 = \mathbf{F}_N^H \Lambda_1 \mathbf{F}_N, \quad \Lambda_1 = i\mu \text{diag}(0, 1, \dots, \frac{N}{2} - 1, 0, 1 - \frac{N}{2}, \dots, -1), \quad (3.2)$$

$$\mathbf{D}_2 = \mathbf{F}_N^H \Lambda_2 \mathbf{F}_N, \quad \Lambda_2 = [\text{i}\mu \text{diag}(0, 1, \dots, \frac{N}{2} - 1, \frac{N}{2}, 1 - \frac{N}{2}, \dots, -1)]^2, \quad (3.3)$$

where \mathbf{F}_N is the discrete Fourier transform matrix with elements $(\mathbf{F}_N)_{j,k} = \frac{1}{\sqrt{N}} e^{-\text{i}jk\frac{2\pi}{N}}$, \mathbf{F}_N^H is the conjugate transpose matrix of \mathbf{F}_N .

Applying the Fourier pseudo-spectral method to the system (2.4) in space, we have

$$\begin{cases} \frac{d}{dt} \mathbf{U} = \mathbf{D} \left(\mathbf{Q} - \mathbf{U}^2 + \mathbf{D}_1 \left((\mathbf{D}_1 \mathbf{U}) \cdot \mathbf{U} \right) \right), \\ \frac{d}{dt} \mathbf{Q} = -\mathbf{U} \cdot \frac{d}{dt} \mathbf{U} - (\mathbf{D}_1 \mathbf{U}) \cdot \left(\mathbf{D}_1 \frac{d}{dt} \mathbf{U} \right), \end{cases} \quad (3.4)$$

where $\mathbf{D} = (\mathbf{I} - \mathbf{D}_2)^{-1} \mathbf{D}_1$, and $\mathbf{U}, \mathbf{Q} \in \mathbb{V}_h$.

Theorem 3.1. *The system (3.4) preserves the following semi-discrete energy conservation law*

$$\frac{d}{dt} E = 0, \quad E = \langle \mathbf{U}, \mathbf{Q} \rangle_h.$$

Proof. Following the semi-discrete system (3.4), we have

$$\begin{aligned} \frac{d}{dt} E &= \left\langle \frac{d}{dt} \mathbf{U}, \mathbf{Q} \right\rangle_h + \left\langle \mathbf{U}, \frac{d}{dt} \mathbf{Q} \right\rangle_h \\ &= \left\langle \frac{d}{dt} \mathbf{U}, \mathbf{Q} \right\rangle_h + \left\langle \mathbf{U}, -\mathbf{U} \cdot \frac{d}{dt} \mathbf{U} - (\mathbf{D}_1 \mathbf{U}) \cdot \left(\mathbf{D}_1 \frac{d}{dt} \mathbf{U} \right) \right\rangle_h \\ &= \left\langle \mathbf{Q} - \mathbf{U}^2 + \mathbf{D}_1 \left((\mathbf{D}_1 \mathbf{U}) \cdot \mathbf{U} \right), \frac{d}{dt} \mathbf{U} \right\rangle_h \\ &= \langle \mathbf{G}, \mathbf{D} \mathbf{G} \rangle_h = 0, \end{aligned}$$

where

$$\mathbf{G} = \mathbf{Q} - \mathbf{U}^2 + \mathbf{D}_1 \left((\mathbf{D}_1 \mathbf{U}) \cdot \mathbf{U} \right),$$

and the last equality follows from the skew-symmetry of \mathbf{D} . \square

Remark 3.1. *If the Fourier pseudo-spectral method is employed for the original system (2.1), we can obtain a new semi-discrete scheme*

$$\frac{d}{dt} \mathbf{U} = \mathbf{D} \left(-\frac{3}{2} \mathbf{U}^2 - \frac{1}{2} (\mathbf{D}_1 \mathbf{U})^2 + \mathbf{D}_1 \left((\mathbf{D}_1 \mathbf{U}) \cdot \mathbf{U} \right) \right), \quad (3.5)$$

which can also be proved to preserve a discrete energy conservation law

$$\frac{d}{dt} H = 0, \quad H = -\frac{h}{2} \sum_{j=0}^{N-1} \left(U_j^3 + U_j \cdot (\mathbf{D}_1 \mathbf{U})_j^2 \right).$$

We note that the energy (2.3) is equivalent to the Hamiltonian energy in continuous sense, but not for the semi-discrete sense.

4 High-order energy-preserving schemes

In this section, we derive two class of high-order energy-preserving schemes by using the RK method and the Gauss collocation method in time for the IEQ reformulated system (3.4), respectively.

Applying an s -stage RK method to solve the system (3.4), we obtain the following scheme.

Scheme 4.1. Let b_i, a_{ij} ($i, j = 1, \dots, s$) be real numbers and $c_i = \sum_{j=1}^s a_{i,j}$. For given $U^n, Q^n \in \mathbb{V}_h$, the following intermediate values are first calculated by

$$U_i = U^n + \tau \sum_{j=1}^s a_{i,j} k_j, \quad (4.1)$$

$$Q_i = Q^n + \tau \sum_{j=1}^s a_{i,j} l_j, \quad (4.2)$$

$$k_i = D \left(Q_i - U_i^2 + D_1 \left((D_1 U_i) \cdot U_i \right) \right), \quad (4.3)$$

$$l_i = -U_i \cdot k_i - (D_1 U_i) \cdot (D_1 k_i), \quad (4.4)$$

where $U_i, Q_i, k_i, l_i \in \mathbb{V}_h$, $i = 1, \dots, s$. Then $U^{n+1}, Q^{n+1} \in \mathbb{V}_h$ is updated via

$$U^{n+1} = U^n + \tau \sum_{i=1}^s b_i k_i, \quad (4.5)$$

$$Q^{n+1} = Q^n + \tau \sum_{i=1}^s b_i l_i. \quad (4.6)$$

The coefficients are given by a Butcher table

$$\begin{array}{c|c} \mathbf{c} & \mathbf{A} \\ \hline & \mathbf{b}^T \end{array} = \begin{array}{c|ccc} c_1 & a_{11} & \cdots & a_{1s} \\ \vdots & \vdots & \ddots & \vdots \\ c_s & a_{s1} & \cdots & a_{ss} \\ \hline & b_1 & \cdots & b_s \end{array},$$

where $\mathbf{A} \in \mathbb{R}^{s,s}$, $\mathbf{b} \in \mathbb{R}^s$, and $\mathbf{c} = \mathbf{A}\mathbf{1}$, with $\mathbf{1} = (1, 1, \dots, 1)^T \in \mathbb{R}^s$.

Applying an s -stage collocation method to (3.4), we obtain the following scheme.

Scheme 4.2. Let c_1, \dots, c_s be distinct real numbers (usually $0 \leq c_i \leq 1$). For given $U^n, Q^n \in \mathbb{V}_h$, $\mathbf{u}(t)$ and $\mathbf{v}(t)$ are two N dimensional vector polynomials of degree s satisfying, respectively,

$$\mathbf{u}(t_n) = U^n, \quad \mathbf{v}(t_n) = Q^n, \quad (4.7)$$

$$\dot{\mathbf{u}}(t_n^i) = D \left(\mathbf{v}(t_n^i) - \mathbf{u}(t_n^i)^2 + D_1 \left((D_1 \mathbf{u}(t_n^i)) \cdot \mathbf{u}(t_n^i) \right) \right), \quad (4.8)$$

$$\dot{\mathbf{v}}(t_n^i) = -\mathbf{u}(t_n^i) \cdot \dot{\mathbf{u}}(t_n^i) - (D_1 \mathbf{u}(t_n^i)) \cdot (D_1 \dot{\mathbf{u}}(t_n^i)), \quad (4.9)$$

where $t_n^i = t_n + c_i \tau$, $i = 1, \dots, s$. And the numerical solution is defined by $U^{n+1} = \mathbf{u}(t_n + \tau)$ and $Q^{n+1} = \mathbf{v}(t_n + \tau)$.

Theorem 1.4 on page 31 of Ref. [22] indicates that the collocation method is equivalent to a RK method. If we take c_1, \dots, c_s as the zeros of the s th shifted Legendre polynomial

$$\frac{d^s}{dx^s} (x^s (x-1)^s),$$

Scheme 4.2 is called Gauss collocation method and has order $2s$, and the zeros are called Gauss collocation points. Collocation points for Gauss collocation methods of order 4 and 6 are given explicitly in Ref. [22].

Theorem 4.1. *The s -stage Gauss collocation Scheme 4.2 is energy-preserving, i.e., it satisfies the following energy conservation law*

$$E^{n+1} = E^n, \quad E^n = \langle \mathbf{U}^n, \mathbf{Q}^n \rangle_h, \quad n = 0, 1, \dots, M-1. \quad (4.10)$$

Proof. It is readily to obtain from Scheme 4.2 that

$$\begin{aligned} E^{n+1} - E^n &= \langle \mathbf{U}^{n+1}, \mathbf{Q}^{n+1} \rangle_h - \langle \mathbf{U}^n, \mathbf{Q}^n \rangle_h = \int_{t_n}^{t_{n+1}} \frac{d}{dt} \langle \mathbf{u}(t), \mathbf{v}(t) \rangle_h dt \\ &= \int_{t_n}^{t_{n+1}} \left(\left\langle \frac{d}{dt} \mathbf{u}(t), \mathbf{v}(t) \right\rangle_h + \left\langle \mathbf{u}(t), \frac{d}{dt} \mathbf{v}(t) \right\rangle_h \right) dt. \end{aligned} \quad (4.11)$$

The integrands $\langle \frac{d}{dt} \mathbf{u}(t), \mathbf{v}(t) \rangle_h$ and $\langle \mathbf{u}(t), \frac{d}{dt} \mathbf{v}(t) \rangle_h$ are polynomials of degree $2s-1$, which are integrated without error by the s -stage Gaussian quadrature formula. It therefore follows from the collocation condition that

$$\begin{aligned} &\int_{t_n}^{t_{n+1}} \left(\left\langle \frac{d}{dt} \mathbf{u}(t), \mathbf{v}(t) \right\rangle_h + \left\langle \mathbf{u}(t), \frac{d}{dt} \mathbf{v}(t) \right\rangle_h \right) dt \\ &= \tau \sum_{i=1}^s b_i \left(\langle \dot{\mathbf{u}}(t_n^i), \mathbf{v}(t_n^i) \rangle_h + \langle \mathbf{u}(t_n^i), \dot{\mathbf{v}}(t_n^i) \rangle_h \right) \\ &= \tau \sum_{i=1}^s b_i \left(\langle \dot{\mathbf{u}}(t_n^i), \mathbf{v}(t_n^i) \rangle_h + \langle \mathbf{u}(t_n^i), -\mathbf{u}(t_n^i) \cdot \dot{\mathbf{u}}(t_n^i) - (\mathbf{D}_1 \mathbf{u}(t_n^i)) \cdot (\mathbf{D}_1 \dot{\mathbf{u}}(t_n^i)) \rangle_h \right) \\ &= \tau \sum_{i=1}^s b_i \langle \mathbf{g}, \dot{\mathbf{u}}(t_n^i) \rangle_h = \tau \sum_{i=1}^s b_i \langle \mathbf{g}, \mathbf{D} \mathbf{g} \rangle_h = 0, \end{aligned} \quad (4.12)$$

where

$$\mathbf{g} = \mathbf{v}(t_n^i) - \mathbf{u}(t_n^i)^2 + \mathbf{D}_1 \left((\mathbf{D}_1 \mathbf{u}(t_n^i)) \cdot \mathbf{u}(t_n^i) \right),$$

and the last equality follows from the skew-symmetry of \mathbf{D} . This completes the proof. \square

For general RK methods, we have following theorem.

Theorem 4.2. *If the coefficients of an s -stage RK Scheme 4.1 satisfy*

$$b_i a_{ij} + b_j a_{ji} = b_i b_j, \quad \forall i, j = 1, \dots, s,$$

then it can preserve the energy conservation law (4.10).

Proof. According to (4.5) and (4.6), we have

$$\begin{aligned} E^{n+1} &= \langle \mathbf{U}^{n+1}, \mathbf{Q}^{n+1} \rangle_h \\ &= \left\langle \mathbf{U}^n + \tau \sum_{i=1}^s b_i k_i, \mathbf{Q}^n + \tau \sum_{j=1}^s b_j l_j \right\rangle_h \\ &= E^n + \tau \sum_{j=1}^s b_j \langle \mathbf{U}^n, l_j \rangle_h + \tau \sum_{i=1}^s b_i \langle k_i, \mathbf{Q}^n \rangle_h + \tau^2 \sum_{i,j=1}^s b_i b_j \langle k_i, l_j \rangle_h. \end{aligned} \quad (4.13)$$

Using (4.1) and (4.2), we obtain

$$\tau \sum_{j=1}^s b_j \langle \mathbf{U}^n, l_j \rangle_h + \tau \sum_{i=1}^s b_i \langle k_i, \mathbf{Q}^n \rangle_h$$

$$\begin{aligned}
&= \tau \sum_{j=1}^s b_j \left\langle U_j - \tau \sum_{i=1}^s a_{j,i} k_i, l_j \right\rangle_h + \tau \sum_{i=1}^s b_i \left\langle k_i, Q_i - \tau \sum_{j=1}^s a_{i,j} l_j \right\rangle_h \\
&= \tau \sum_{i=1}^s b_i \left(\left\langle U_i, l_i \right\rangle_h + \left\langle Q_i, k_i \right\rangle_h \right) - \tau^2 \sum_{i,j=1}^s (b_i a_{i,j} + b_j a_{j,i}) \left\langle k_i, l_j \right\rangle_h.
\end{aligned} \tag{4.14}$$

It follows from (4.13) and (4.14) that

$$E^{n+1} = E^n + \tau \sum_{i=1}^s b_i \left(\left\langle U_i, l_i \right\rangle_h + \left\langle Q_i, k_i \right\rangle_h \right), \tag{4.15}$$

where $b_i a_{ij} + b_j a_{ji} = b_i b_j$ was used. Note that

$$\begin{aligned}
\left\langle U_i, l_i \right\rangle_h + \left\langle Q_i, k_i \right\rangle_h &= \left\langle U_i, -U_i \cdot k_i - (D_1 U_i) \cdot (D_1 k_i) \right\rangle_h + \left\langle Q_i, k_i \right\rangle_h \\
&= \left\langle Q_i - U_i^2 + D_1 \left((D_1 U_i) \cdot U_i \right), k_i \right\rangle_h \\
&= 0,
\end{aligned}$$

where the last equality follows from (4.3) and the skew-symmetry of D . Thus, we obtain

$$E^{n+1} = E^n, \quad n = 0, 1, \dots, M-1.$$

This completes the proof. \square

Remark 4.1. *To the best of our knowledge, there has been no reference considering a second-order, linear-implicit and energy-preserving scheme for the CH equation by using the IEQ approach. Thus, in Appendix A, we investigate such scheme.*

5 Numerical examples

In this section, we will investigate the accuracy, CPU time and invariants-preserving of the proposed schemes. Theoretically, the newly proposed high-order schemes 4.1 and 4.2 could reach arbitrarily high-order accuracy in time (with proper choice of the Gauss collocation points), and they all can exactly preserve the discrete energy (4.10). For simplicity, in the rest of this paper, the Gauss methods of order 4 (denoted by HIEQ-GCS $s = 2$) and 6 (denoted by HIEQ-GCS $s = 3$) are only used for demonstration purposes. Also, the results are compared with the energy-preserving Fourier pseudo-spectral scheme (denoted by EPFPS) and the multi-symplectic Fourier pseudo-spectral scheme (denoted by MSFPS), where we substitute the Fourier pseudo-spectral method into the wavelet collocation method for space directions in Refs. [18] and [44], respectively. For the convergence rate, we use the formula

$$\text{Rate} = \frac{\ln(\text{error}_1/\text{error}_2)}{\ln(\tau_1/\tau_2)},$$

where τ_l, error_l , ($l = 1, 2$) are step sizes and errors with the step size τ_l , respectively.

5.1 Accuracy test

We consider the periodic smooth solution with the initial condition

$$u_0(x) = \sin(x), \quad x \in \Omega = [0, 2\pi],$$

and the periodic boundary condition. The *exact* solution is obtained numerically by HIEQ-GCS $s = 3$ under a very small time step $\tau = 0.001$ and spatial step $h = \frac{2\pi}{128}$ at $T = 1$. In Tables 1 and 2, we display the numerical error in discrete L^∞ -norm and the convergence rate for different schemes at $T = 1$, respectively. As illustrated in Table 1, all of the schemes have second-order convergence rate in time, and from table 2, it is clear to see that HIEQ-GCS $s = 2$ and HIEQ-GCS $s = 3$ can arrive at fourth-order and sixth-order convergence rates in time, respectively. In Fig. 1, we plot the global numerical error in discrete L^∞ -norm versus the CPU time for different schemes. The plot shows that, for a given global error, the sixth-order scheme is computationally cheapest. The IEQ-LCNS admits larger numerical errors than the ones provided by EPFPS and MSFPS, however, it is computationally cheaper.

Table. 1: The numerical error and convergence rate for different second-order schemes with $h = \frac{2\pi}{128}$ and different time steps at $T = 1$.

Scheme	τ	L^∞	Rate
IEQ-LCNS	$\frac{1}{100}$	2.083e-04	-
	$\frac{1}{200}$	5.182e-05	2.01
	$\frac{1}{400}$	1.293e-05	2.00
	$\frac{1}{800}$	3.230e-06	2.00
	$\frac{1}{1600}$	8.075e-07	2.00
EPFPS	$\frac{1}{100}$	4.354e-05	-
	$\frac{1}{200}$	1.089e-05	2.00
	$\frac{1}{400}$	2.722e-06	2.00
	$\frac{1}{800}$	6.806e-07	2.00
	$\frac{1}{1600}$	1.701e-07	2.00
MSFPS	$\frac{1}{100}$	4.344e-05	-
	$\frac{1}{200}$	1.086e-05	2.00
	$\frac{1}{400}$	2.716e-06	2.00
	$\frac{1}{800}$	6.790e-07	2.00
	$\frac{1}{1600}$	1.697e-07	2.00

Table. 2: The numerical error and convergence rate for different high-order schemes with $h = \frac{2\pi}{128}$ and different time steps at $T = 1$.

Scheme	τ	L^∞	Rate
HIEQ-GCS $s = 2$	$\frac{1}{30}$	2.817e-07	-
	$\frac{1}{60}$	1.765e-08	4.00
	$\frac{1}{120}$	1.104e-09	4.00
	$\frac{1}{240}$	6.900e-11	4.00
HIEQ-GCS $s = 3$	$\frac{1}{30}$	2.231e-010	-
	$\frac{1}{60}$	3.523e-012	5.98
	$\frac{1}{120}$	5.534e-014	5.99
	$\frac{1}{240}$	8.854e-016	5.99

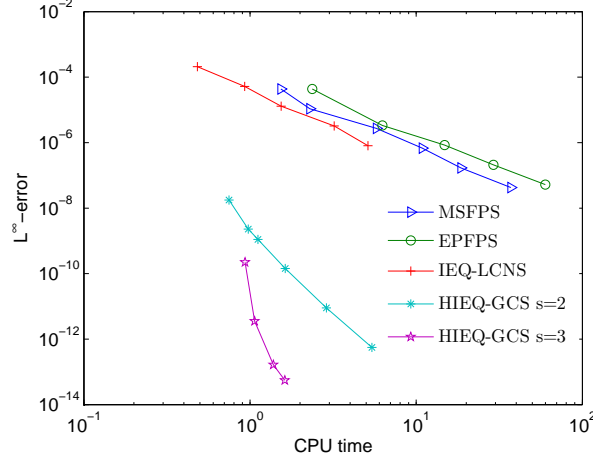


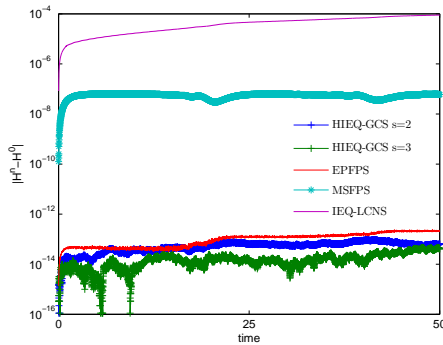
Fig. 1: The numerical error versus the CPU time.

5.2 Peakon solution

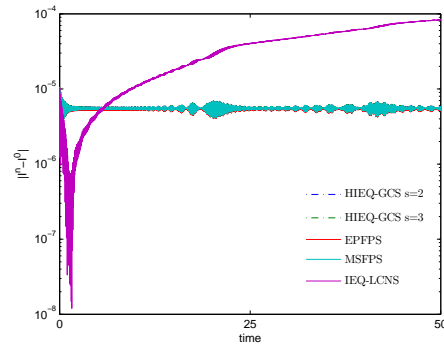
We consider the periodic peaked traveling wave with the initial condition [40]

$$u_0(x) = \begin{cases} \frac{c}{\cosh(L/2)} \cosh(x - x_0), & |x - x_0| \leq L/2, \\ \frac{c}{\cosh(L/2)} \cosh(L - (x - x_0)), & |x - x_0| > L/2, \end{cases}$$

where c is the wave speed, L is the period, and x_0 is the position of the trough. In the numerical experiment, the parameters are chosen as $c = 1$, $L = 1$, and $x_0 = 0$ and the periodic boundary condition is considered. The errors of invariants are plotted in Fig. 2. In Fig. 2 (a), we can see that IEQ-LCNS and MSFPS can only preserve the Hamiltonian energy approximately and the error provided by IEQ-LCNS is largest. In theory, the proposed high-order schemes cannot exactly preserve the discrete Hamiltonian energy, but, from Fig. 2 (b), we can observe that the resulting errors provided by HIEQ-GCS $s = 2$ and HIEQ-GCS $s = 3$, respectively, can be preserved up to the machine accuracy and are much smaller than the one provided by EPFPS. In Figs. 2 (c)-2 (f), it is clear to see that the errors of the momentum are bounded and all of the schemes can exactly preserve the mass conservation law. Figs. 2 (g)-2 (h) show that the proposed schemes can exactly preserve the discrete energy conservation law (4.10), which conforms the theoretical analysis.



(a) Hamiltonian energy errors



(b) Momentum errors

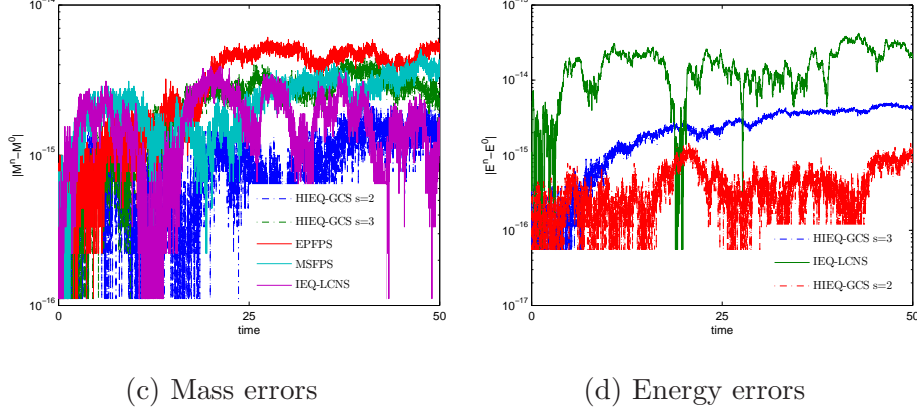


Fig. 2: The errors in invariants with $h = \frac{L}{128}$ and $\tau = 0.0001$ over the time interval $t \in [0, 50]$.

5.3 Three-peakon interaction

In this example, we consider the three-peakon interaction of the CH equation with the initial condition [40]

$$u_0(x) = \phi_1(x) + \phi_2(x) + \phi_3(x),$$

where

$$\phi_i(x) = \begin{cases} \frac{c_i}{\cosh(L/2)} \cosh(x - x_i), & |x - x_i| \leq L/2, \\ \frac{c_i}{\cosh(L/2)} \cosh(L - (x - x_i)), & |x - x_i| > L/2, \end{cases} \quad i = 1, 2, 3.$$

The parameters are $c_1 = 2, c_2 = 1, c_3 = 0.8, x_1 = -5, x_2 = -3, x_3 = -1$ and $L = 30$, and the computational domain is $\Omega = [0, L]$ with the periodic boundary condition. In Fig. 3, we display the interaction of three peakons by HIEQ-GCS $s = 2$ at $t = 0, 1, 2, 3, 4, 6, 8$ and 10, respectively. We can see clearly that the moving peakon interaction is resolved very well. The three-peakon interaction obtained by other schemes are not presented since they are close to figure 3. The errors of invariants are plotted in Fig. 4, which shows that all of the schemes can exactly preserve the mass conservation law and the momentum errors provided by the schemes are bounded. The Hamiltonian energy errors provided by the high-order schemes are smallest and the newly proposed schemes can exactly preserve the discrete energy conservation law (4.10).

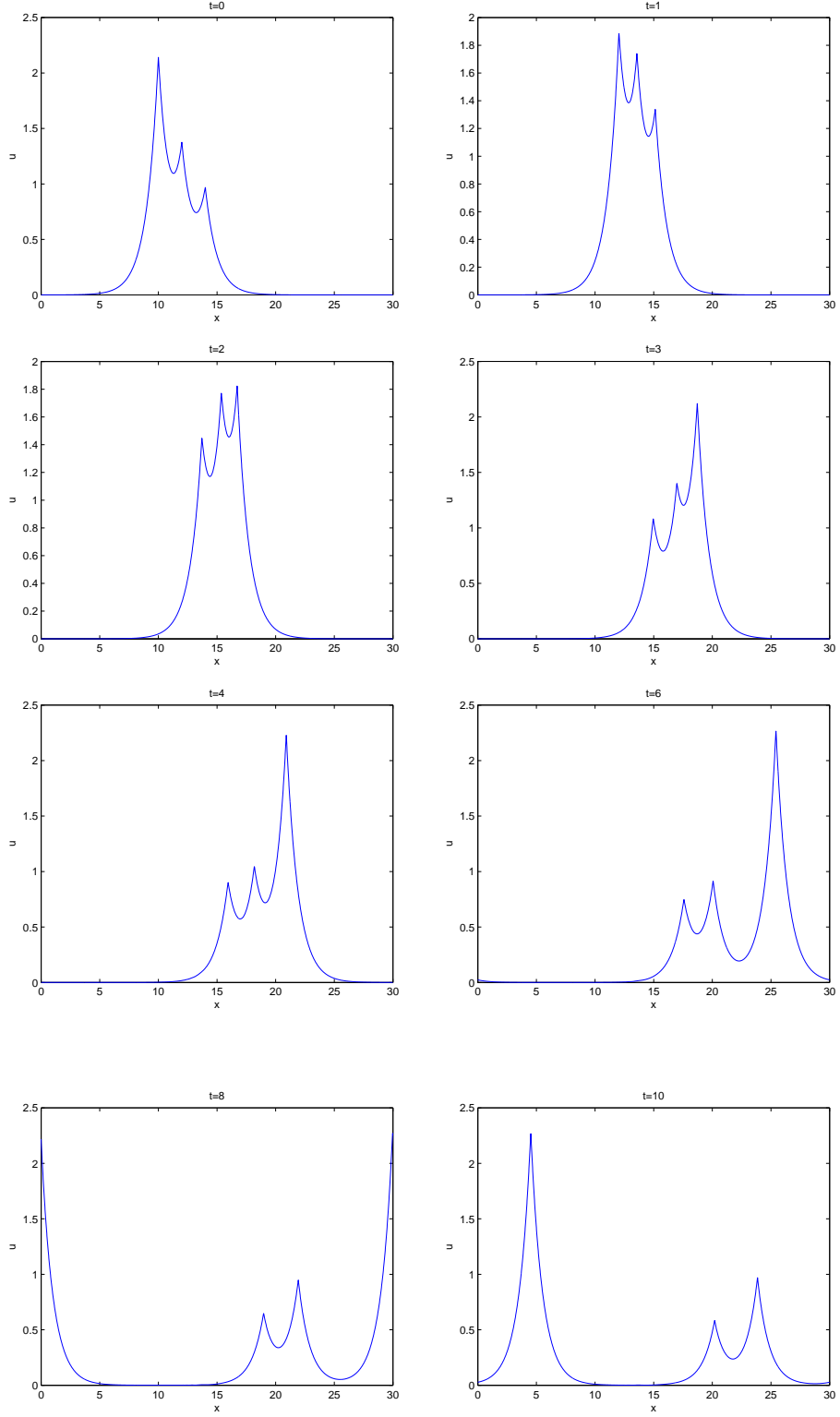


Fig. 3: The three-peakon interaction of the CH equation (1.1) provided by HIEQ-GCS $s = 2$, $h = \frac{L}{2048}$ and $\tau = 0.0001$ at $t = 0, 1, 2, 3, 4, 6, 8$ and 10 , respectively.

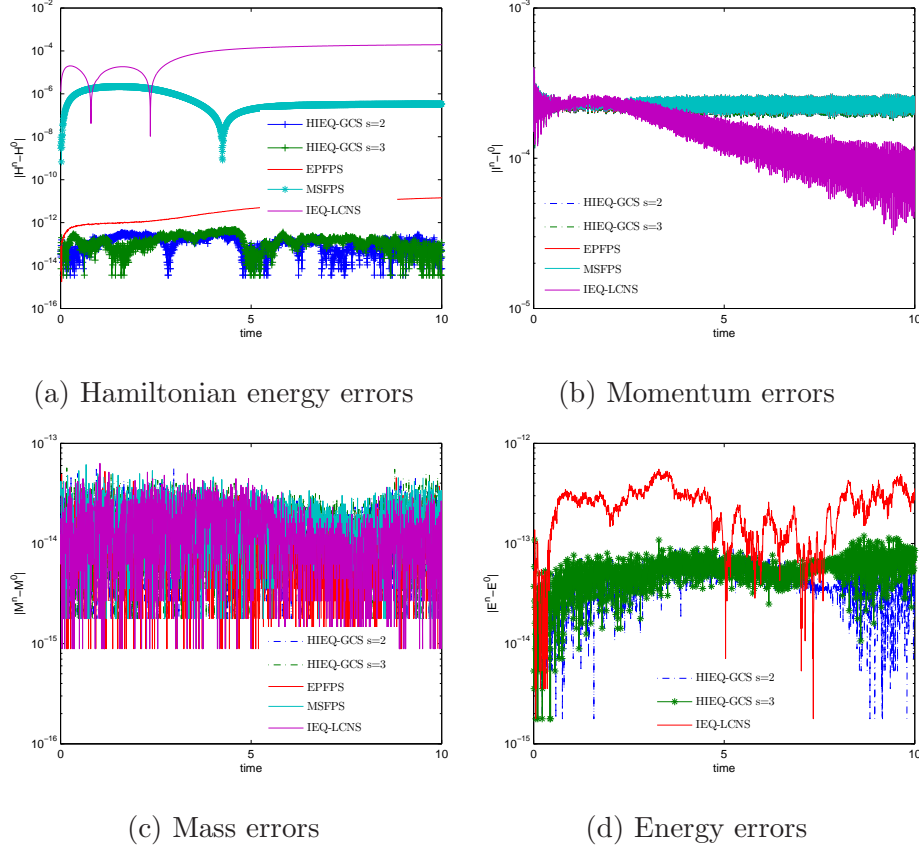


Fig. 4: The errors in invariants with $h = \frac{L}{2048}$ and $\tau = 0.0001$ over the time interval $t \in [0, 10]$.

6 Concluding remarks

In this paper, we combine the IEQ approach with structure-preserving methods to propose a new class of energy-preserving methods for the CH equation. The proposed schemes could reach arbitrarily high-order accuracy while exactly preserving the discrete energy conservation law. Numerical examples are addressed to illustrate the accuracy and energy-preserving property of the proposed schemes. Compared with some existing low-order structure-preserving schemes, the proposed high-order schemes show remarkable efficiency and the advantage in preserving the discrete Hamiltonian energy. The technique presented in this paper can also be used to construct high-order energy-preserving methods for other Hamiltonian PDEs, such as the KdV equation, the Schrödinger equation, the Klein-Gordon-Schrödinger equations, etc. In addition, we can also apply the scalar auxiliary variable (SAV) approach [36, 37] to reformulate the CH equation into an equivalent form with a quadratic energy functional. Thus, how to combine the SAV approach with structure-preserving methods to derive high-order energy-preserving methods for Hamiltonian PDEs will be our future work.

Acknowledgments

This work is supported by the National Natural Science Foundation of China (Grant Nos. 11771213, 11801269), the National Key Research and Development Project of China (Grant Nos. 2016YFC0600310, 2018YFC0603500), the Major Projects of Natural Sciences of University in Jiangsu Province of China (Grant No. 15KJA110002), the

Natural Science Foundation of Jiangsu Province (Grant no. BK20180413), the Priority Academic Program Development of Jiangsu Higher Education Institutions, the Natural Science Foundation of the Jiangsu Higher Education Institutions of China (Grant no. 18KJB110015) and the foundation of Jiangsu Key Laboratory for Numerical Simulation of Large Scale Complex Systems (201905).

Appendix:

A A novel linear-implicitly and energy-preserving scheme

In this section, inspired by Refs. [19, 25], we develop a novel, linear-implicit and energy-preserving scheme for the CH equation by utilizing the linearized Crank-Nicolson method to discretize the semi-discrete system (3.4) in time. The resulting scheme is denoted by IEQ-LCNS.

Scheme A.1. (*IEQ-LCNS*) Applying the linearized Crank-Nicolson method to discretize the semi-discrete system (3.4) in time, we obtain a fully discretized scheme, as follows:

$$\begin{cases} \delta_t^+ U^n = D \left(Q^{n+\frac{1}{2}} + \text{diag}(-\hat{U}^{n+\frac{1}{2}}) U^{n+\frac{1}{2}} \right. \\ \quad \left. - D_1 \left(\text{diag}(-D_1 \hat{U}^{n+\frac{1}{2}}) U^{n+\frac{1}{2}} \right) \right), \\ \delta_t^+ Q^n = \text{diag}(-\hat{U}^{n+\frac{1}{2}}) \delta_t^+ U^n + \text{diag}(-D_1 \hat{U}^{n+\frac{1}{2}}) D_1 \delta_t^+ U^n. \end{cases} \quad (\text{A.1})$$

where $\delta_t U^n = \frac{U^{n+1} - U^n}{\tau}$, $\hat{U}^{n+\frac{1}{2}} = \frac{3U^n - U^{n-1}}{2}$ and $Q^{n+\frac{1}{2}} = \frac{Q^{n+1} + Q^n}{2}$ and U^1, Q^1 is the solution of the following equation

$$\begin{cases} \delta_t^+ U^0 = D \left(Q^{\frac{1}{2}} + \text{diag}(-U^0) U^{\frac{1}{2}} - D_1 \left(\text{diag}(-D_1 U^0) U^{\frac{1}{2}} \right) \right), \\ \delta_t^+ Q^0 = \text{diag}(-U^0) \delta_t^+ U^0 + \text{diag}(-D_1 U^0) D_1 \delta_t^+ U^0. \end{cases} \quad (\text{A.2})$$

Theorem A.1. The IEQ-LCN scheme (A.1)-(A.2) can exactly preserve the discrete energy conservation law (4.10).

Proof. We can deduce from (A.1) that

$$\begin{aligned} \delta_t^+ \langle Q^n, U^n \rangle_h &= \langle \delta_t^+ Q^n, U^{n+\frac{1}{2}} \rangle_h + \langle Q^{n+\frac{1}{2}}, \delta_t^+ U^n \rangle_h \\ &= \langle \text{diag}(-\hat{U}^{n+\frac{1}{2}}) \delta_t^+ U^n + \text{diag}(-D_1 \hat{U}^{n+\frac{1}{2}}) D_1 \delta_t^+ U^n, U^{n+\frac{1}{2}} \rangle_h \\ &\quad + \langle Q^{n+\frac{1}{2}}, \delta_t^+ U^n \rangle_h \\ &= \langle \text{diag}(-\hat{U}^{n+\frac{1}{2}}) U^{n+\frac{1}{2}} - D_1 (\text{diag}(-D_1 \hat{U}^{n+\frac{1}{2}}) U^{n+\frac{1}{2}}), \delta_t^+ U^n \rangle_h \\ &\quad + \langle Q^{n+\frac{1}{2}}, \delta_t^+ U^n \rangle_h \\ &= \langle G^n, \delta_t^+ U^n \rangle_h = \langle G^n, D G^n \rangle_h = 0, \end{aligned} \quad (\text{A.3})$$

where

$$G^n = Q^{n+\frac{1}{2}} + \text{diag}(-\hat{U}^{n+\frac{1}{2}}) U^{n+\frac{1}{2}} - D_1 (\text{diag}(-D_1 \hat{U}^{n+\frac{1}{2}}) U^{n+\frac{1}{2}}),$$

and the last equality follows from the skew-symmetry of D . Thus, according to (A.3), we have

$$E^{n+1} = E^n, \quad E^n = \langle Q^n, U^n \rangle_h, \quad n = 1, 2, \dots, M-1.$$

An argument similar to (A.2) used in (A.3) shows that

$$E^1 = E^0.$$

This completes the proof. \square

Subsequently, we show that the above scheme can be solved efficiently. Indeed, we first rewrite (A.1) as

$$\begin{cases} \mathbf{U}^{n+\frac{1}{2}} = \mathbf{U}^n + \frac{\tau}{2} \mathbf{D} \left[\mathbf{Q}^{n+\frac{1}{2}} + \mathbf{g}_1^n \mathbf{U}^{n+\frac{1}{2}} \right], \\ \mathbf{Q}^{n+\frac{1}{2}} = \mathbf{g}_2^n \mathbf{U}^{n+\frac{1}{2}} + \mathbf{Q}^n - \mathbf{g}_2^n \mathbf{U}^n, \end{cases} \quad (\text{A.4})$$

where

$$\begin{aligned} \mathbf{g}_1^n &= \text{diag}(-\hat{\mathbf{U}}^{n+\frac{1}{2}}) - \mathbf{D}_1 \left(\text{diag}(-\mathbf{D}_1 \hat{\mathbf{U}}^{n+\frac{1}{2}}) \right), \\ \mathbf{g}_2^n &= \text{diag}(-\hat{\mathbf{U}}^{n+\frac{1}{2}}) + \text{diag}(-\mathbf{D}_1 \hat{\mathbf{U}}^{n+\frac{1}{2}}) \mathbf{D}_1. \end{aligned}$$

Then, by eliminating $\mathbf{Q}^{n+\frac{1}{2}}$ from (A.4), we have

$$\mathbf{U}^{n+\frac{1}{2}} = \frac{\tau}{2} \mathbf{D} \left[\mathbf{g}_1^n \mathbf{U}^{n+\frac{1}{2}} + \mathbf{g}_2^n \mathbf{U}^{n+\frac{1}{2}} \right] + \mathbf{b}^n, \quad (\text{A.5})$$

where

$$\mathbf{b}^n = \mathbf{U}^n + \frac{\tau}{2} \mathbf{D} \left(\mathbf{Q}^n - \mathbf{g}_2^n \mathbf{U}^n \right).$$

Finally, we obtain $\mathbf{U}^{n+\frac{1}{2}}$ from (A.5) by using the following iteration method for linear equations (A.5)

$$\mathbf{U}^{n+\frac{1}{2},s+1} = \frac{\tau}{2} \mathbf{D} \left[\mathbf{g}_1^n \mathbf{U}^{n+\frac{1}{2},s} + \mathbf{g}_2^n \mathbf{U}^{n+\frac{1}{2},s} \right] + \mathbf{b}^n, \quad (\text{A.6})$$

where we take the initial iteration vector $\mathbf{U}^{n+\frac{1}{2},0} = \mathbf{U}^n$ and each iteration will terminate if the infinity norm of the error between two adjacent iterative steps is less than 10^{-14} . Then, $\mathbf{Q}^{n+\frac{1}{2}}$ is obtained from the first equality of (A.4). Subsequently, we have $\mathbf{U}^{n+1} = 2\mathbf{U}^{n+\frac{1}{2}} - \mathbf{U}^n$ and $\mathbf{Q}^{n+1} = 2\mathbf{Q}^{n+\frac{1}{2}} - \mathbf{Q}^n$.

Remark A.1. We should note from (A.5) that, the IEQ approach need introduce an auxiliary variable, but the auxiliary variable can be eliminated in practical computations.

References

- [1] L. Brugnano, M. Calvo, J.I. Montijano, and L. Rndez. Energy-preserving methods for Poisson systems. *J. Comput. Appl. Math.*, 236:3890–3904, 2012.
- [2] L. Brugnano and F. Iavernaro. *Line Integral Methods for Conservative Problems*. Chapman et Hall/CRC: Boca Raton, FL, USA, 2016.
- [3] L. Brugnano, F. Iavernaro, and D. Trigiante. Hamiltonian boundary value methods (energy preserving discrete line integral methods). *J. Numer. Anal. Ind. Appl. Math.*, 5:17–37, 2010.

- [4] J. Cai, J. Hong, Y. Wang, and Y. Gong. Two energy-conserved splitting methods for three-dimensional time-domain Maxwell's equations and the convergence analysis. *SIAM. J. Numer. Anal.*, 53:1918–1940, 2015.
- [5] W. Cai, Y. Sun, and Y. Wang. Geometric numerical integration for peakon b-family equations. *Commun. Comput. Phys.*, 19:24–52, 2016.
- [6] R. Camassa and D. Holm. An integrable shallow water equation with peaked solitons. *Phys. Rev. Lett.*, 71:1661–1664, 1993.
- [7] R. Camassa, D. Holm, and J. Hyman. A new integrable shallow water equation. *Adv. Appl. Mech.*, 31:1–33, 1994.
- [8] R. Camassa and L. Lee. Complete integrable particle methods and the recurrence of initial states for a nonlinear shallow-water wave equation. *J. Comput. Phys.*, 227:7206–7221, 2008.
- [9] J. Chen and M. Qin. Multi-symplectic Fourier pseudospectral method for the nonlinear Schrödinger equation. *Electr. Trans. Numer. Anal.*, 12:193–204, 2001.
- [10] G. Coclite, K. Karlsen, and N. Risebro. A convergent finite difference scheme for the Camassa-Holm equation with general H^1 initial data. *SIAM J. Numer. Anal.*, 46:1554–1579, 2008.
- [11] D. Cohen and E. Hairer. Linear energy-preserving integrators for Poisson systems. *BIT*, 51:91–101, 2011.
- [12] D. Cohen, B. Owren, and X. Raynaud. Multi-symplectic integration of the Camassa-Holm equation. *J. Comput. Phys.*, 227:5492–5512, 2008.
- [13] D. Cohen and X. Raynaud. Geometric finite difference schemes for the generalized hyperelastic-rod wave equation. *J. Comput. Appl. Math.*, 235:1925–1940, 2011.
- [14] A. Constantin and J. Escher. Global existence and blow-up for a shallow water equation. *Ann. Scuola Norm. Sup. Pisa Cl. Sci.*, 26:303–328, 1998.
- [15] S. Eidnes, L. Li, and S. Sato. Linearly implicit structure-preserving schemes for Hamiltonian systems. *arXiv preprint arXiv:1901.03573*, 2019.
- [16] B. Feng and Y. Liu. An operator splitting method for the Degasperis-Procesi equation. *J. Comput. Phys.*, 228:7805–7820, 2009.
- [17] B. Feng, K. Maruno, and Y. Ohta. A self-adaptive moving mesh method for the Camassa-Holm equation. *J. Comput. Appl. Math.*, 235:229–243, 2010.
- [18] Y. Gong and Y. Wang. An energy-preserving wavelet collocation method for general multi-symplectic formulations of Hamiltonian PDEs. *Commun. Comput. Phys.*, 20:1313–1339, 2016.
- [19] Y. Gong, Y. Wang, and Q. Wang. Linear-implicit conservative schemes based on energy quadratization for Hamiltonian PDEs. *Preprint*.
- [20] Y. Gong, J. Zhao, X. Yang, and Q. Wang. Fully discrete second-order linear schemes for hydrodynamic phase field models of binary viscous fluid flows with variable densities. *SIAM J. Sci. Comput.*, 40:B138–B167, 2018.
- [21] E. Hairer. Energy-preserving variant of collocation methods. *J. Numer. Anal. Ind. Appl. Math.*, 5:73–84, 2010.

- [22] E. Hairer, C. Lubich, and G. Wanner. *Geometric Numerical Integration: Structure-Preserving Algorithms for Ordinary Differential Equations*. Springer-Verlag, Berlin, 2nd edition, 2006.
- [23] H. Holden and X. Raynaud. Convergence of a finite difference scheme for the Camassa-Holm equation. *SIAM J. Numer. Anal.*, 44:1655–1680, 2006.
- [24] Q. Hong, Y. Gong, and Z. Lv. Linear and Hamiltonian-conserving Fourier pseudo-spectral schemes for the Camassa-Holm equation. *Appl. Math. Comput.*, 346:86–95, 2019.
- [25] C. Jiang, W. Cai, and Y. Wang. A linear-implicit and energy-preserving scheme for the sine-Gordon equation based on the invariant energy quadratization approach. *arXiv preprint arXiv:1808.06854*, 2018.
- [26] C. Jiang, W. Cai, Y. Wang, and H. Li. A sixth order energy-conserved method for three-dimensional time-domain Maxwell’s equations. *arXiv preprint, arXiv:1705.08125*, 2017.
- [27] H. Kalisch and J. Lenells. Numerical study of traveling-wave solutions for the Camassa-Holm equation. *Chaos Solitons Fractals*, 25:287–298, 2005.
- [28] A. Li and P. Olver. Well-posedness and blow-up solutions for an integrable nonlinearly dispersive model wave equation. *J. Differ. Equ.*, 162:27–63, 2000.
- [29] H. Li, Y. Wang, and M. Qin. A sixth order averaged vector field method. *J. Comput. Math.*, 34:479–498, 2016.
- [30] Y. Li and X. Wu. Functionally fitted energy-preserving methods for solving oscillatory nonlinear Hamiltonian systems. *SIAM J. Numer. Anal.*, 54:2036–2059, 2016.
- [31] T. Matsuo. A Hamiltonian-conserving Galerkin scheme for the Camassa-Holm equation. *J. Comput. Appl. Math.*, 234:1258–1266, 2010.
- [32] T. Matsuo and H. Yamaguchi. An energy-conserving Galerkin scheme for a class of nonlinear dispersive equations. *J. Comput. Phys.*, 228:4346–4358, 2009.
- [33] Y. Miyatake. An energy-preserving exponentially-fitted continuous stage Runge-Kutta method for Hamiltonian systems. *BIT*, 54:777–799, 2014.
- [34] G.R.W. Quispel and D.I. McLaren. A new class of energy-preserving numerical integration methods. *J. Phys. A: Math. Theor.*, 41:045206, 2008.
- [35] J. Shen and T. Tang. *Spectral and High-Order Methods with Applications*. Science Press, Beijing, 2006.
- [36] J. Shen, J. Xu, and J. Yang. A new class of efficient and robust energy stable schemes for gradient flows. *arXiv:1710.01331*, 2017.
- [37] J. Shen, J. Xu, and J. Yang. The scalar auxiliary variable (SAV) approach for gradient. *J. Comput. Phys.*, 353:407–416, 2018.
- [38] W. Tang and Y. Sun. Time finite element methods: a unified framework for numerical discretizations of ODEs. *Appl. Math. Comput.*, 219:2158–2179, 2012.
- [39] B. Wang and X. Wu. Functionally-fitted energy-preserving integrators for Poisson systems. *J. Comput. Phys.*, 364:137–152, 2018.

- [40] Y. Xu and C.-W Shu. A local discontinuous Galerkin method for the Camassa-Holm equation,. *SIAM J. Numer. Anal.*, 46:1998–2021, 2008.
- [41] X. Yang, J. Zhao, and Q. Wang. Numerical approximations for the molecular beam epitaxial growth model based on the invariant energy quadratization method. *J. Comput. Phys.*, 333:104–127, 2017.
- [42] X. Yang, J. Zhao, Q. Wang, and J. Shen. Numerical approximations for a three components Cahn-Hilliard phase-field model based on the invariant energy quadratization method. *Math. Models Methods Appl. Sci.*, 27:1993–2030, 2017.
- [43] J. Zhao, X. Yang, Y. Gong, and Q. Wang. A novel linear second order unconditionally energy stable scheme for a hydrodynamic-tensor model of liquid crystals. *Comput. Methods Appl. Mech. Engrg.*, 318:803–825, 2017.
- [44] H. Zhu, S. Song, and Y. Tang. Multi-symplectic wavelet collocation method for the Schrödinger equation and the Camassa-Holm equation. *Comput. Phys. Comm.*, 182:616–627, 2011.